Astronomy & Astrophysics

Chemical compositions of four B-type supergiants in the SMC wing

J.-K. Lee, W. R. J. Rolleston, P. L. Dufton, and R. S. I. Ryans

Department of Pure & Applied Physics, The Queen's University of Belfast, BT7 1NN, Northern Ireland, UK
e-mail: j.k.lee@qub.ac.uk

Abstract. High-resolution UCLES/AAT spectra of four B-type supergiants in the SMC South East Wing have been analysed using non-LTE model atmosphere techniques to determine their atmospheric parameters and chemical compositions. The principle aim of this analysis was to determine whether the very low metal abundances (-1.1 dex compared with Galactic value) previously found in the Magellanic Inter Cloud region (ICR) were also present in the SMC Wing. The chemical compositions of the four targets are similar to those found in other SMC objects and appear to be incompatible with those deduced previously for the ICR. Given the close proximity of the Wing to the ICR, this is difficult to understand and some possible explanations are briefly discussed.

Key words. galaxies: Magellanic Clouds – stars: abundances – stars: early-type – stars: supergiants

1. Introduction

Between the Large (LMC) and Small (SMC) Magellanic Clouds, two satellite galaxies of our own Milky Way, lies a column of gas known as the Magellanic Bridge. This Bridge greatly exceeds the galaxies' tidal limit, and is widely considered to be a remnant of the gravitational interactions between the Magellanic Clouds and the Milky Way. Numerical simulations by, for example, Gardiner & Noguchi (1996) and Sawa et al. (1999) imply that the tidal effects from a close encounter of the two Magellanic Clouds about ~200 Myr ago produced a tidal bridge and tail structure and subsequently triggered an episode of star formation. This tail/bridge structure is believed to constitute the inter-cloud region (ICR) and would be seen as overlapping in the sky, with the tail material modeled to be more distant than the bridge and with a larger radial velocity (Gardiner & Noguchi 1996). The SMC wing is located to the east of the SMC and enveloped by neutral hydrogen gas (see Fig. 2). In optical images it appears as a large cloud of faint stars extending 6.5° eastward from the SMC toward the LMC, and contains young stellar component (e.g. Westerlund & Glaspey 1971; Kunkel 1980) that indicates recent star formation history. According to the predictions of the models (Kunkel et al. 1994), this Wing constitutes the densest regions of the bridge/tail material along the line-of-sight.

The tail/bridge material, if it is indeed the product of the past encounter(s) of the Clouds, would be expected to have the metallicity of its progenitors. However, a recent study by Rolleston et al. (1999) of 3 B-type dwarfs in the ICR reported that they had a metallicity lower by -1.1 dex than that of our Galaxy, and this is also significantly lower than the values found for the SMC and LMC (e.g. Korn et al. 2000; Kurt et al. 1999; Rolleston et al. 1993, 1996, 2003; Venn 1999). A possible explanation is that the inter-cloud material could have been stripped off from either of the galaxies at a much earlier encounter (about ~8 Gyr ago; Kobulnicky & Skillman 1997; Da Costa & Hatzidimitriou 1998), when less nucleo-synthetic processing of interstellar medium (ISM) of the SMC had occurred. However, this would be inconsistent with the numerical simulations discussed above that imply this ICR was formed relatively recently and also with the presence of early-type stars.

Here we attempt to confirm and extend the results of Rolleston et al. by investigating the chemical composition of the SMC wing. Using intermediate dispersion spectroscopy, we have identified suitable targets and here present high-resolution spectroscopy of four of these objects. By investigating the metallicity of these stars, we can address questions concerning the chemical homogeneity, or inhomogeneity, of the two distinct components, as well as possibly the tidal origin of the SMC wing material.

2. Observations and data reduction

The high-resolution spectroscopic data presented here were obtained during two observing runs with the 3.9-m Anglo-Australian Telescope (AAT) in October 1999 and 2000. The University College of London Échelle Spectrograph (UCLES) was used with the 31 lines mm^{-1} grating and with

Table 1. Observational summary of the four program stars.

Star	RA, Dec (2000.0)	V [mag]	AAT/ UCLES	T_{exp} [s]	v_{lsr} [km s^{-1}]	S/N
ICR 02134-7431	02 13 26, −74 31 20	12.3	1999-10-25	7500	+197	80
SK 194	01 45 03, −74 31 32	11.7	2000-10-14	6600	+214	140
SK 202	01 53 03, −73 55 30	12.3	2000-10-14	25 200	+180	125
SK 213	02 09 30, −74 26 00	13.7	2000-10-16	7200	+203	60

a TeK 1K × 1K CCD, providing complete spectral coverage between $\lambda\lambda$3900–4900 Å at a *FWHM* resolution of ~0.1 Å. Stellar exposures were divided into either 1200 or 1500 s segments with the total observing times being listed in Table 1. These exposure times should be treated with some caution as the observing conditions varied significantly during the two observing runs. Stellar exposures were bracketed with Cu–Ar arc exposures for wavelength calibration.

The two dimensional CCD datasets were reduced using standard procedures within IRAF (Tody 1986). Preliminary processing of the CCD frames such as over-scan correction, trimming of the data section and flat-fielding were performed using the CCDRED package (Massey 1997), whilst cosmic-ray removal, extraction of the stellar spectra, sky-subtraction and wavelength calibration were carried out using the SPECRED (Massey et al. 1992) and DOECSLIT (Willmarth & Barnes 1994) packages. The spectra were then co-added and re-binned to 0.1 Å, which was adequate for the relatively broad metal absorption lines (with typical full-width-half-maximum widths of 1–2 Å) found in these supergiant spectra. The signal-to-noise (*S/N*) ratios found in the continuum are summarized in Table 1 for a wavelength of approximately 4300 Å. Note that care has been taken to include different parts of the blaze profile in these measurements so that they should be representative of the overall quality of the spectra. In Fig. 1, we illustrate the quality of the spectra for the region 4465–4485 Å, which was chosen as it contains lines of He I and Mg II observable in all four targets. For the hottest star, SK 213, the Mg II line is relatively weak, with an equivalent width of approximately 70 mÅ but is still clearly visible. Indeed lines with equivalent widths greater than 40 mÅ could be measured in all our targets with weaker features being identified in the two targets with the highest *S/N* ratios.

Heliocentric stellar radial velocities (summarised in Table 1) and equivalent widths (*EW*s) of lines were measured using the STARLINK spectrum analysis program DIPSO (Howarth et al. 1994). Low order polynomials were used to represent the adjacent continuum regions for normalisation and then Gaussian profiles were fitted to the metal and non-diffuse helium lines using non-linear least square routines. As discussed by Ryans et al. (2003), the profiles of metal absorption lines in the spectra of early-type supergiants are well represented by a Gaussian profile but tests using a different profile shape showed that this assumption was not critical. For hydrogen lines, the above method was not feasible as there was insufficient continuum regions for normalisation. Instead the continua of the adjacent orders were moved to a common
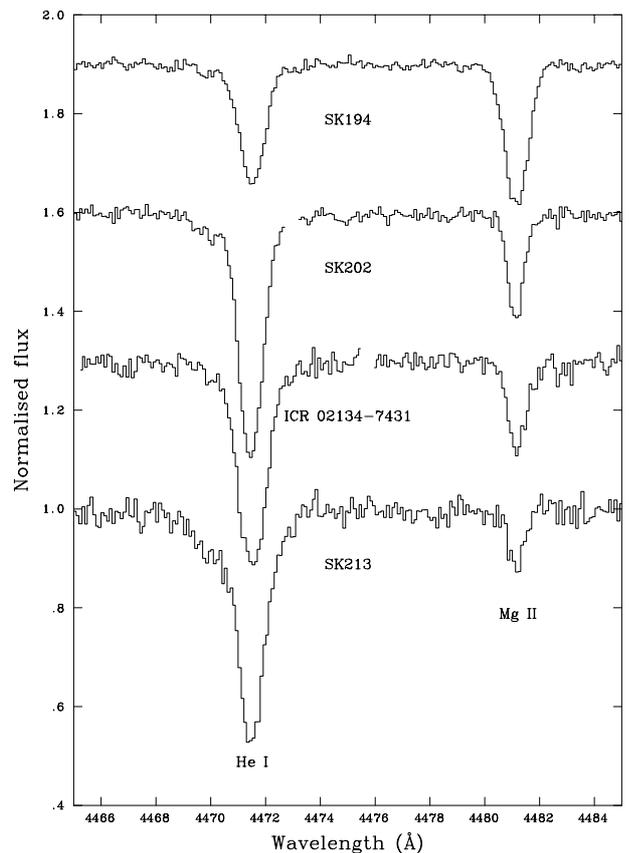

Fig. 1. Normalised spectra of the 4 targets covering the region 4465 to 4485 Å, containing a He I and a Mg II line. The spectra were re-binned to a pixel size of 0.1 Å. In SK 213 the Mg II line has an equivalent width of approximately 70 mÅ.

wavelength scale, fitted by low order polynomials, which were then merged. This estimate of the blaze profile was then used to rectify the order containing the hydrogen lines. Profiles were then extracted with the continuum levels being defined at ±16 Å from the line centre.

3. Model atmospheres

3.1. Model atmosphere calculations

The analysis is based on grids of non-LTE model atmosphere calculated using the codes TLUSTY and SYNSPEC (Hubeny 1988; Hubeny & Lanz 1995; Hubeny et al. 1998). Details of the methods can be found in Ryans et al. (2003), while the grids will be discussed in more detail by Dufton et al. (2005).
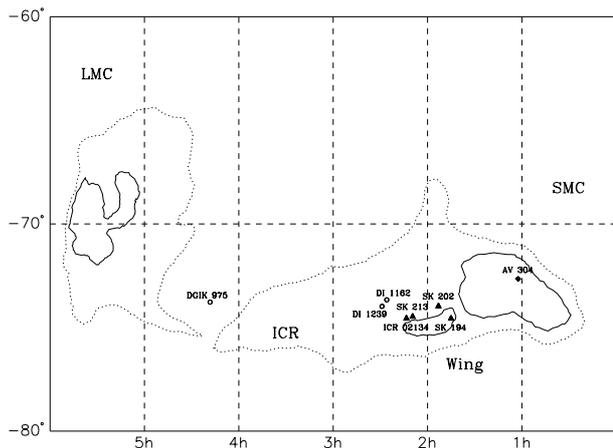
Fig. 2. Schematic diagram of the LMC, SMC and the Inter-Cloud Region. Solid lines define the stellar concentrations within the Magellanic Clouds, while the dashed lines show the H I envelopes of the Magellanic system. The positions of our targets within the SMC wing are marked by solid black triangles. Other targets have been discussed by Rolleston et al. (1999, circles; 2003, diamond).

Briefly four grids are being generated with base metallicities corresponding to our galaxy ($\left[\frac{Fe}{H}\right]$ = 7.5 dex) and with metallicities reduced by 0.3, 0.6 and 1.1 dex. These lower metallicities were chosen so as to be representative of the LMC, SMC and ICR material. For each base metallicity, approximately 3000 models have been calculated covering a range of effective temperature from 12 000 to 35 000 K, logarithmic gravities (in cm s^{-2}) from 4.5 dex down to close to the Eddington limit (which will depend on the effective temperature) and microturbulences of 0, 5, 10, 20 and 30 km s^{-1}. Then for any set of atmospheric parameters, five models were calculated keeping the iron abundance fixed but allowing the light element (e.g. C, N, O, Mg, Si) abundances to vary from +0.8 dex to −0.8 dex around their base values. Effectively this approaches assumes that the line blanketing and atmospheric structure is dominated by iron and hence that the light element abundances can be varied without significantly affecting this structure. Tests discussed in Dufton et al. (2005) appear to confirm that this approach is reasonable.

These models are then used to calculate spectra, which in turn provide theoretical hydrogen and helium line profiles and equivalent widths for light metals for a range of abundances. Note that as we keep the iron abundance fixed within any given grid, we have less extensive data for this element. The theoretical equivalent widths are then available via a GUI interface written in IDL, which allows the user to interpolate in order to calculate equivalent widths and/or abundance estimates for approximately 200 metal lines for any given set of atmospheric parameters. Ryans et al. (2003) reported that the increments of 0.4 dex used in our grids were fine enough to ensure that no significant errors were introduced by the interpolation procedures. Full theoretical spectra are also available for any given model. Details of the model grids, atomic data used in the line strength calculations and wavelength ranges used in the equivalent width calculations are available at `http://star.pst.qub.ac.uk/`. In summary these grids

Table 2. Atmospheric parameters of the program stars derived for two microturbulences (v_t), 10 and 20 km s^{-1}, using the SMC and ICR model grids. Each pair of effective temperature (in K) and logarithmic gravity (in cm s^{-2}) is written as numbers separated by a comma.

v_t	IC 02134-7431	SK 202	SK 213	SK 194
	SMC grid			
10	15 000, 2.1	14 750, 2.2	20 000, 2.9	11 700, 1.7
20	14 750, 2.1	14 750, 2.2	20 500, 2.9	11 500, 1.7
	ICR grid			
10	15 000, 2.1	14 750, 2.2	21 000, 2.9	12 000, 1.7
20	14 750, 2.1	14 750, 2.2	20 750, 2.9	11 500, 1.7

allow a user-friendly non-LTE analysis of hydrogen and helium line profiles and of the profiles and equivalent width of the lines of light elements over a range of iron line blanketing and atmospheric parameters appropriate to B-type stars in our Galaxy and in Local Group galaxies such as the Magellanic Clouds.

During the analysis, one of the program stars, SK 194, was found to have atmospheric parameters below our lowest grid points in both effective temperature and surface gravity. We have therefore calculated additional models for T_{eff} = 11 000 K and $\log g$ = 1.6 to enable the spectrum of this star to be analysed.

3.2. Estimation of atmospheric parameters

The estimation of atmospheric parameters involves an iterative process as they are interrelated. Firstly adopting appropriate values of the surface gravity (using the calibration of McErlean et al. 1999), the effective temperature was estimated using the ionisation balances due to silicon. For the coolest star, SK 194, only one ionization level of silicon was observed, in this case the He I line profiles were used to estimate the effective temperature. Although the helium lines are very sensitive to effective temperature in this regime, this method implicitly assumes that the helium abundance of SK 194 is normal. Using these preliminary effective temperature estimates, the surface gravities were then estimated by comparing the observed hydrogen Balmer line profiles with theoretical calculations. These new gravity estimates were used as the starting point in the next iteration to estimate effective temperatures, and the process was repeated until convergence was obtained. The entire procedure was undertaken for both v_t = 10 and 20 km s^{-1}, consistent with the microturbulences found for supergiants by Gies & Lambert (1992), McErlean et al. (1999) and Trundle et al. (2004).

As discussed above, the ionisation balance of silicon lines was used for IC 02134-7431 and SK 202 which show both Si II and III lines. For SK 213 whose observed spectra exhibited only Si III lines, the absence of Si II and Si IV lines was respectively used to provide constraints on the lower and upper limit to the effective temperature. The mean of the derived lower and upper limits (which differed by <1000 K) was taken to be the effective temperature of the star. The derived parameters are summarised in Table 2, using the grids with an iron abundance of 6.9 dex (SMC grid) and 6.4 dex (ICR grid).

Table 3. Absolute abundances of the program stars in the TLUSTY SMC grid for two microturbulences, 10 and 20 km s^{-1}. The last three columns present results of three other recent studies of SMC stars (see text).

| | ICR 02134-7431 | | SK 202 | | SK 213 | | SK 194 | | SMC supergiants | | AV 304 |
	VT10	VT20	VT10	VT20	VT10	VT20	VT10	VT20	TLPD	DRTLHL	
C II	6.7	6.7 (1)	6.8	6.8 (1)	7.2	7.2 (2)	–	–	7.30	7.06	7.36
N II	7.4	7.3 (1)	7.6	7.4 (2)	7.7	7.6 (9)	7.9	8.0(1)	7.67	7.42	6.55
O II	–	–	–	–	8.3	8.0 (15)	–	–	8.15	8.09	8.13
Mg II	6.7	6.6 (1)	6.6	6.5 (1)	6.7	6.7 (1)	6.8	6.6(1)	6.78	6.79	6.77
Si II/III	6.7	6.6 (4)	6.9	6.8 (4)	7.2	6.7 (3)	7.1	6.8(2)	6.74	6.85	6.76
Fe II	–	–	–	–	–	–	6.2	6.1(15)	–	–	–

3.3. Photospheric abundances

The adopted atmospheric parameters (listed in Table 2) were used to derive absolute non-LTE abundances from the observed equivalent widths for the programme stars. The grids with iron abundance appropriate to either the SMC or ICR were used (together with the appropriate atmospheric parameters) but as the differences in the abundance estimates were small only the results for the SMC grid are presented in Table 3.

4. Discussion

The absolute abundances of metallic lines are summarised in Table 3 on a logarithmic scale with [H] ≡ 12.0 dex. An observational uncertainty of ±10 mÅ in the equivalent width estimate of an individual line would change an abundance estimate by typically ±0.15 dex. Where several lines due to an ionic species are observed the corresponding error in the mean abundance would be expected to be smaller. The abundance estimates may also be affected by errors in the adopted atmospheric parameters. The results, presented in Table 3 for microturbulences of $v_t = 10$ and 20 km s^{-1}, lead to changes in the abundance estimates of typically ±0.1 dex, with larger uncertainties for in a few cases. For the effective temperature and gravity, numerical tests adopting error estimates of ±1000 K and ±0.2 dex respectively, lead to changes in the abundance estimates of typically 0.1 to 0.3 dex. Finally there will be uncertainties due to the intrinsic assumptions made in the model atmosphere calculations and in particular the neglect of the stellar wind. However, Trundle et al. (2004) have used the non-LTE unified model atmosphere code FASTWIND first introduced by Santolaya-Rey et al. (1997) to analyse the spectra of SMC supergiants. For two targets, these results have been compared with those deduced using TLUSTY (see Dufton et al. 2005) and the comparison indicates that the neglect of the wind may not be a serious source of error. Hence we conclude that an error estimate of ±0.3 dex might be appropriate to our abundance estimates.

The main purpose of this analysis is to investigate whether the very low metal abundances for the ICR found by Rolleston et al. (1999) are also present in our SMC wing targets. To provide a comparison for our results, we have utilised three other recent studies of hot stars in the SMC. Trundle et al. (2004, TLPD) studied 7 supergiants using the non-LTE unified model atmosphere code FASTWIND. Dufton et al. (2005)

have undertaken analysis of 9 supergiants using the same non-LTE grids as adopted here. As discussed above, the two analyses yield similar results for two targets in common indicating that both TLPD and Dufton et al. should form suitable comparisons. Lennon et al. (2003) corrected the LTE analysis of AV 304, a sharp lined B0V star, of Rolleston et al. (2003) in order to allow for non-LTE effects. Although these corrections can only be approximate, they would appear to provide estimates that agree well with a full non-LTE analysis currently being undertaken by the authors. The results of all these analyses are summarized in Table 3, the first two being for stars at a similar evolutionary to our targets, whilst the third should reflect the current chemical composition of the SMC interstellar medium. The three analyses yield different N (and to a lesser extent O) abundances estimates for reasons that are discussed below. However the excellent agreement for the O, Mg and Si abundances provide indirect support for their use as comparators for our SMC wing targets. Below we briefly discuss the estimates obtained for each element.

– **Carbon:** The carbon abundances in the Wing targets appear to be lower for ICR 02134-7431 and SK 202 than for other SMC targets. The value for SK 213 appear relatively normal, whilst no C II features were measurable in SK 194. However these results must be treated with caution for the estimates have used the doublet at 4267 Å. As discussed by, for example, Sigut (1996), this element suffers from significant non-LTE effects which are difficult to model. Additionally, Lennon et al. (2003) found that, even in a non-LTE analysis, this doublet appears to yield lower abundance estimates (by 0.3–0.4 dex) than is found from other C II lines. Indeed the carbon abundance for AV 304 presented in Table 3 has been corrected for this effect and this may explain the difference between the C abundance estimates in Dufton et al. (2005) and for AV 304. Hence we do not believe that there is any significant evidence for the carbon abundance of our Wing targets being lower than that for the SMC in general.

– **Nitrogen:** Nitrogen abundances were found for all four targets and range from 7.3 to 8.0 dex. TLPD also found a significant variation in their abundance estimates that they ascribed to different degrees of contamination by nucleosynthetically processed material. This is also consistent with the far larger nitrogen abundances found in the supergiant samples than in AV 304 or in analysis of SMC H II regions (see, for example, Kurt et al. 1999). Hence the N abundance

Table 4. A non-LTE analysis of the ICR stars using TLUSTY. For each star, the newly derived atmospheric parameters are followed by their absolute abudances along with the differential abundances relative to AV 304. Where more than one lines were used in the analysis, the standard deviation of the sample is ≲0.3 dex.

	DI 1162		DI 1239		DGIK 975	
T_{eff} [K]	21 500		24 500		21 000	
$\log g$ [cm]	3.25		3.70		3.35	
v_{t} [km s^{-1}]	5		5		5	
C II	7.2 (2)	−0.3 (2)	7.5	+0.2	<6.8 (2)	<−0.6 (2)
N II	6.5	−0.1	<7.3 (2)	<+0.5	6.5	−0.1
O II	7.8 (6)	−0.3 (6)	7.6 (11)	−0.5 (10)	7.9 (10)	−0.2 (10)
Mg II	6.3	−0.5	6.3	−0.4	6.0	−0.8
Si II/III	6.5 (5)	−0.5 (3)	6.0 (3)	−0.8 (3)	6.2 (5)	−0.9 (3)
Mean[*]		**−0.4 ± 0.2**		**−0.4 ± 0.4**		**−0.6 ± 0.3**

[*] Excluing N.

estimates for our targets appear to be compatible with those for other evolved SMC supergiants.

– **Oxygen:** The O II spectrum is only observed in our hottest target with the abundance estimates being sensitive to the adopted microturbulence. However they are consistent with those found in other SMC B-type stars.

– **Magnesium:** All the abundance estimates are based on the Mg II doublet at 4481 Å. However they show little variation and are in excellent agreement with the other analyses.

– **Silicon:** These abundance estimates are based on both Si II and Si III features. However, as the silicon ionization equilibrium has been used to constrain the effective temperature, the results have been combined into a single abundance estimate for each star. For our hottest target, SK 213, the results are affected by the choice of microturbulence but in general the estimates are compatible with other analyses of SMC objects.

The principle conclusion from the model atmosphere analysis is that the SMC Wing targets appear to have similar chemical compositions to those of other objects in the SMC. In particular there is no evidence for the low metallicity found in the ICR targets by Rolleston et al. (1999). From Fig. 2, it can be seen that all four targets are close to the inter-cloud region and it is arguable that two targets (ICR 02134-7431 and SK 213) are indeed part of the ICR or at the boundary between the Wing and the ICR. Given this close proximity, the difference in the chemical composition found by Rolleston et al. and in the present study is surprising especially as the ICR is thought to have formed from material from the SMC and LMC. The low metallicity found by Rolleston et al. implies that the most likely source of the material is the SMC and then one is forced to the conclusion that the ICR originated from a region close to (or indeed part of) the Wing but with a different chemical composition to that found for the parts of the Wing that we have sampled.

An alternative explanation is that the results in Rolleston et al. are unreliable and that the ICR has a metallicity consistent with the SMC (or LMC). The low metallicity of the ICR was based on an LTE analysis of three targets with effective temperature in the range 20 000 to 24 000 K and logarithmic gravities of 3.6 to 3.8 dex; this would correspond to a spectral classification of early-B-type giants/dwarfs. The analysis was undertaken differentially with respect to two galactic stars with very similar atmospheric parameters, whilst the hottest ICR target (DI 1239) was also analysed relative to the SMC main sequence star AV 304, which has an effective temperature approximately 2500 K higher. The results for all three stars were consistent and indicated that the metallicity of the ICR was between 1.0 and 1.2 dex lower than our Galaxy for the elements C, N, O, Mg and Si. Additionally the abundances of O, Mg and Si were found to be 0.5 to 0.7 dex lower in DI 1239 compared with AV 304. One of the principal areas of uncertainty in the Rolleston et al. analysis was the use an LTE approximation.

To investigate this, we have re-analysed the ICR stars in Rolleston et al. (1999) using the same non-LTE grids used in this study. The atmospheric parameters were re-deduced using the same methodology adopted by Rolleston et al., i.e. the effective temperature was derived using the Balmer discontinuity and the surface gravity from the comparison of the observed Balmer line profiles with the non-LTE theoretical spectra. Using these new atmospheric parameters, we have derived the absolute non-LTE abundance of the ICR stars and detailed line-by-line differential abundances relative to AV 304 (summary in Table 4). While the non-LTE atmospheic parameters are different from their LTE counterparts, the derived absolute abundances agree very well with the corresponding LTE values within the error. So do the differential abudances relative to the SMC standard AV 304. More importantly, the metal deficiency seen in Rolleston et al. is still evident in our non-LTE analysis. With an exception of C and N for which the ICR stars show both over- and under-abundances, other metal lines (O, Mg and Si) all show similar amount of underabundace as seen in Rolleston et al. Rolleston et al. reported the ICR stars have metallicity ∼−0.5 dex lower than that of

the SMC. Excluding N, which might have been contaminated from the dredged-up material, the average of our differential analysis gives a similar value.

The other main uncertainty is probably the choice of the microturbence. This quantity is difficult to estimate and its choice would affect the stronger metal lines in the Galactic stellar spectra more than those for the ICR targets. Hence, for example, adoption of larger microturbulences would reduce the magnitude of the underabundance found in the ICR. However, the microturbulences found by Rolleston et al. from the O II spectra range from 5 to 10 km s^{-1} and appear reasonable for the stellar atmospheric parameters (see, for example, Hardorp & Scholz 1970; Gies & Lambert 1992; Kilian et al. 1994).

Lehner et al. (2001) has studied the interstellar ultraviolet absorption and H I emission spectrum towards a young star in Magellanic Bridge. These observations also appeared to support a low metallicity ($\simeq -1.1$ dex) compared to that of the Galaxy. Hence, although the failure to identify a low metallicity component in the SMC Wing is worrying, there would appear to be no substantial reason to discount the results of Rolleston et al. (1999). Clearly further observations of targets in both the ICR and the SMC/ICR interface are crucial to understanding this discrepancy.

References

Da Costa, G. S., & Hatzidimitriou, D. 1998, AJ, 115, 1934

Dufton, P. L., Ryans, R. S. I., Trundle, C., et al. 2005, A&A, in preparation

Gardiner, L. T., & Noguchi, M. 1996, MNRAS, 278, 191

Gies, D. L., & Lambert, D. L. 1992, ApJ, 387, 673

Hardorp, J., & Scholz, M. 1970, ApJ, 154, 1111

Howarth, I. D., Murray, M. J., & Mills, D. 1994, Starlink User Note, No. 50

Hubeny, I. 1988, Computer Physics Comm., 52, 103

Hubeny, I., & Lanz, T. 1995, ApJ, 439, 875

Hubeny, I., Heap, S. R., & Lanz, T. 1998, in Properties of Hot, Luminous Stars, Boulder-Munich, ed. I. D. Howarth, ASP Conf. Ser., 131, 108

Kilian, J., Montenbruch, O., & Nissen, P. E. 1994, A&A, 284, 37

Korn, A. J., Becker, S. R., Gummersbach, C. A., & Wolf, B. 2000, A&A, 385, 143

Kobulnicky, H. A., & Skillman, E. D. 1997, ApJ, 489, 636

Kunkel, W. E. 1980, in Star Formation, IAU Symp., 85, 353

Kunkel, W. E., Demers, S., & Irwin, M. J. 1994, in The Local Group: Comparative and Global Properties, 200

Kurt, C. M., Dufour, R. J., Garnett, D. R., et al. 1999, ApJ, 518, 246

Lehner, N., Sembach, K. R., Dufton, P. L., Rolleston, W. R. J., & Keenan, F. P. 2001, ApJ, 551, 781

Lennon, D. J., Dufton, P. L., & Crowley, C. 1999, A&A, 398, 455

McErlean, N. D., Lennon, D. J., & Dufton, P. L. 1999, A&A, 349, 553

Massey, P. 1997, A User's Guide to Reducing Slit Spectra with IRAF, NOAO Laboratory

Massey, P., Valdes, F., & Barnes, J. 1994, A User's Guide to CCD Reductions with IRAF, NOAO Laboratory

Rolleston, W. J. R., Dufton, P. L., Fitzsimmons, A., Howarth, I. D., & Irwin, M. J. 1993, A&A, 277, 10

Rolleston, W. J. R., Brown, P. J. F., Dufton, P. L., & Howarth, I. D. 1996, A&A, 315, 95

Rolleston, W. J. R., Dufton, P. L., McErlean, N. D., & Venn, K. A. 1999, A&A, 348, 728

Rolleston, W. J. R., Venn, K. A., Tolstoy, E., & Dufton, P. L. 2003, A&A, 400, 21

Ryans, R. S. I., Dufton, P. L., Rolleston, W. J. R., et al. 2002, MNRAS, 336, 577

Ryans, R. S. I., Dufton, P. L., Mooney, C. J., et al. 2003, A&A, 401, 1119

Santolaya-Rey, A. E., Puls, J., & Herrero, A. 1997, A&A, 323, 488

Sawa, T., Fujimoto, M., & Kumai, Y. 1999, in New Views of the Magellanic Cloud, IAU Symp., 190, 499

Sigut, T. A. A. 1996, ApJ, 473, 452

Tody, D. 1986, IRAF User Manual, NOAO Laboratory

Trundle, C., Lennon, D. J., Puls, J., & Dufton, P. L. 2004, A&A, 417, 217

Venn, K. A. 1999, ApJ, 518, 405

Westerlund, B. E., & Glaspey, J. 1971, A&A, 10, 1

Willmarth, D., & Barnes, J. 1994, A User's Guide to Reducing Echelle Spectra with IRAF, NOAO Laboratory